# Supporting Information

# Lasing in Ni Nanodisk Arrays

Sara Pourjamal,[†] Tommi K. Hakala,[*,†,‡] Marek Nečada,[†] Francisco Freire-Fernández,[†] Mikko Kataja,[†,¶] Heikki Rekola,[§] Jani-Petri Martikainen,[†] Päivi Törmä,[†] and Sebastiaan van Dijken[*,†]

†*Department of Applied Physics, Aalto University School of Science, FI-00076 Aalto, Finland*

‡*Institute of Photonics, University of Eastern Finland, FI-80101 Joensuu, Finland*

¶*Institut de Ciència de Materials de Barcelona (ICMAB-CSIC), Campus de la UAB, Bellaterra, Catalonia, Spain*

§*Smart Photonic Materials, Faculty of Engineering and Natural Sciences, Tampere University, P.O. Box 541, FI-33101 Tampere, Finland*

E-mail: tommi.hakala@uef.fi; sebastiaan.van.dijken@aalto.fi

## 1 Ni Nanodisk Array Transmission Curves

Figure S1 shows transmission curves for Ni nanodisk arrays with $p_x = 380\,\text{nm}$ and $p_y$ ranging from 370 nm to 390 nm. The intensity maxima are close to the DOs of the lattice. For incident polarization along $y$, the DO wavelength is given by $\lambda = n \times p_x = 578\,\text{nm}$. The DO for incident polarization along $x$ scales with $p_y$ and, thus, it red-shifts from (a) to (e). The strong decrease of the transmission intensity beyond the DO is characteristic for the excitation of a SLR mode. In lasing experiments, we observe intense lasing peaks just above

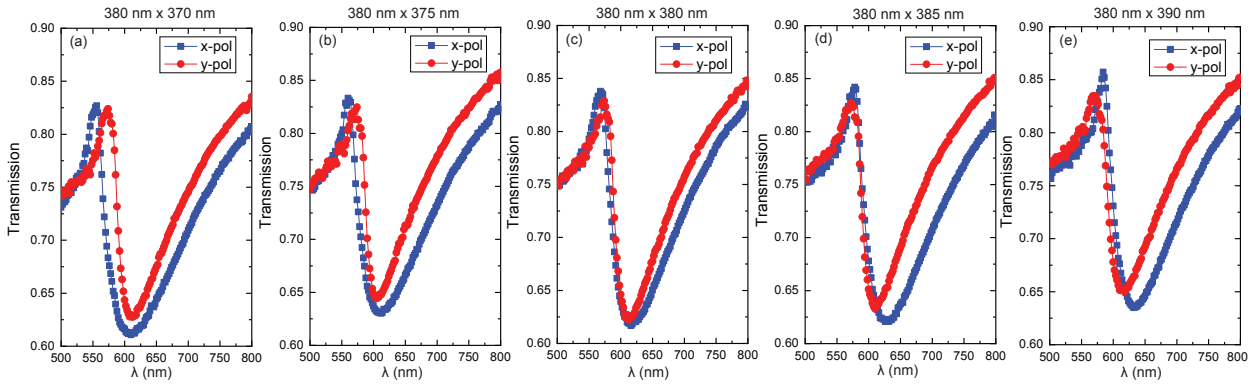


Figure S1: Experimental transmission curves for Ni nanodisk arrays with $p_x = 380\,\text{nm}$ and $p_y$ ranging from 370 nm to 390 nm. Results for incident polarization along $x$ and $y$ are shown.

the DO wavelengths where the R6G dye solution can emit to a SLR mode of the Ni nanodisk array.

## 2 Lasing Simulations

We modelled lasing using the Lumerical FDTD software. The gain material was chosen as a four level medium with level lifetimes defined as in Figure S2. We modified the Lumerical build-in 4-level gain material by adding also the possibility of non-radiative decay from the upper lasing level to the ground state. We note that it had only a minor effect on the results. For the gain material we used lifetime parameters $\tau_{30} = 1\,\text{ns}$, $\tau_{32} = 100\,\text{fs}$, $\tau_{21} = 3\,\text{ns}$, $\tau_{10} = 100\,\text{fs}$, and $\tau_{20} = 240\,\text{ps}$. Of these parameters, the precise values of $\tau_{32}$ and $\tau_{10}$ were not important as long as they were short so that inversion could develop quickly. Non-radiative decay described by $\tau_{20}$ was also not important because faster lasing dynamics dominated the behavior. The position and width of the emission and absorption lines were $\omega_e = 2.178\,\text{eV}$, $\gamma_e = 0.1014\,\text{eV}$ and $\omega_a = 2.428\,\text{eV}$, $\gamma_a = 0.215\,\text{eV}$, respectively.[1]

Pumping was done well above the lasing threshold with a 100 fs laser pulse centered at 500 nm wavelength traveling orthogonal to the array plane with various polarizations. We set the thickness of the gain material to 300 nm and the refractive index of the surroundings to $n = 1.52$. Periodic boundary conditions were applied along $x$ and $y$ while a perfectly matched

layer surrounded the system along the $z$-axis. In the lasing simulations, we considered an array with $p_x = 380$ nm and $p_y = 370$ nm.

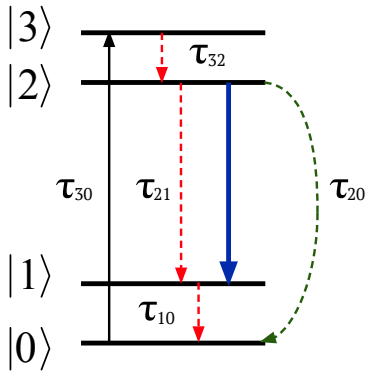


Figure S2: Schematic illustration of the 4-level gain material in our lasing simulations with corresponding lifetime parameters.

If the system is pumped with $x$- or $y$-polarized light, the simulations indicate lasing at wavelengths that match the positions of the experimentally observed lasing peaks. However, these simulations do not reproduce two-mode lasing. We do attain two-mode lasing when the polarization of the pump pulse is set to a 45° angle (Figure S3). This could indicate that our inability to model angled injection in FDTD simulations with a gain material might be at fault. Interestingly, the simulation with 45° polarization suggests that the lasing peak at lower wavelength is broader, while simulations with $x$- and $y$-polarized pump pulses do not suggest such asymmetry. This result may point to a complex interplay between partly overlapping modes that share the same gain material.

In Figure S3 we also demonstrate the magnitude of material dependencies. In addition to simulations with Ni nanoparticles, we simulated an otherwise identical array with Au nanoparticles. We find similar linewidths for the lasing peaks in both systems, but the relative strengths of the lasing lines are different. Furthermore, the lasing peak at lower wavelength is somewhat blue-shifted for the Au nanoparticles.

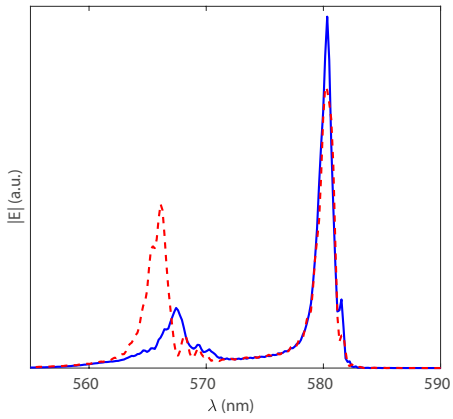


Figure S3: Simulated lasing spectra for 380 nm × 370 nm arrays with pump polarization at a 45° angle. The spectra show the averaged electric field in the transmission plane 900 nm from the array. Spectra are calculated for Ni (blue solid line) and Au nanoparticles (red dashed line).

# 3 Measurements of Pump and Polarization Dependent Emission Spectra

We performed measurements on all Ni nanodisk arrays with 15 different pump fluences and 3 settings of the output polarization filter ($x$ filter, $y$ filter, no filter). Figure S4 shows logarithmic plots of emission spectra at $k_y = 0$ for each pump fluence. Figure S5 illustrates the lasing threshold behavior of $p_x$ ($\lambda \approx 580$ nm) and $p_y$ (varying $\lambda$) related modes.

In rectangular arrays, the lasing output at $p_y$ related wavelengths is strictly $x$ polarized, i.e., the output polarization copies the pump polarization, while at the $p_x$ related wavelength, the polarization of the lasing output depends on particle periodicity and pump fluence. We observe nontrivial dynamics above the threshold, where some lasing peaks tend to broaden and split upon a further increase of laser power. This behavior is an indication of mode competition. Typically, the $p_x$ related peak starts to appear near the DO crossing and it spreads towards slightly higher wavelength with increasing pump fluence. For all arrays except 380 nm × 390 nm, this peak has both $x$ and $y$ polarization components at the onset of lasing. For the 380 nm × 370 nm array at the highest pump fluence and for the 380 nm × 390 nm

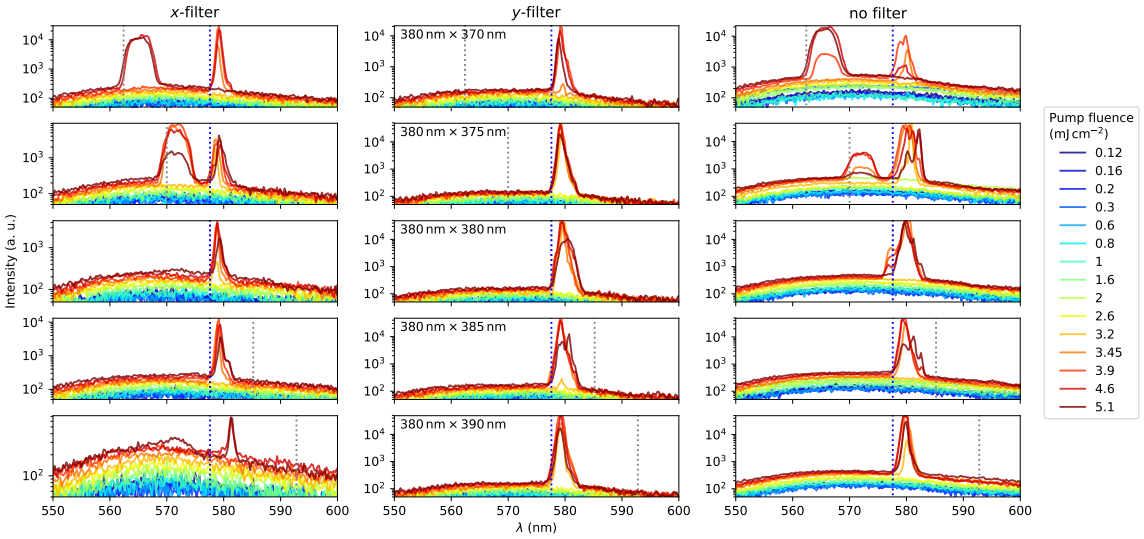


Figure S4: Pump fluence dependence of emission spectra at $k_y = 0$ for samples having $p_x = 380\,\text{nm}$ and $p_y$ ranging from 370 nm to 390 nm. Polarization of the lasing output is analyzed with an $x$ filter (left column), $y$ filter (center column), or no filter (right column).

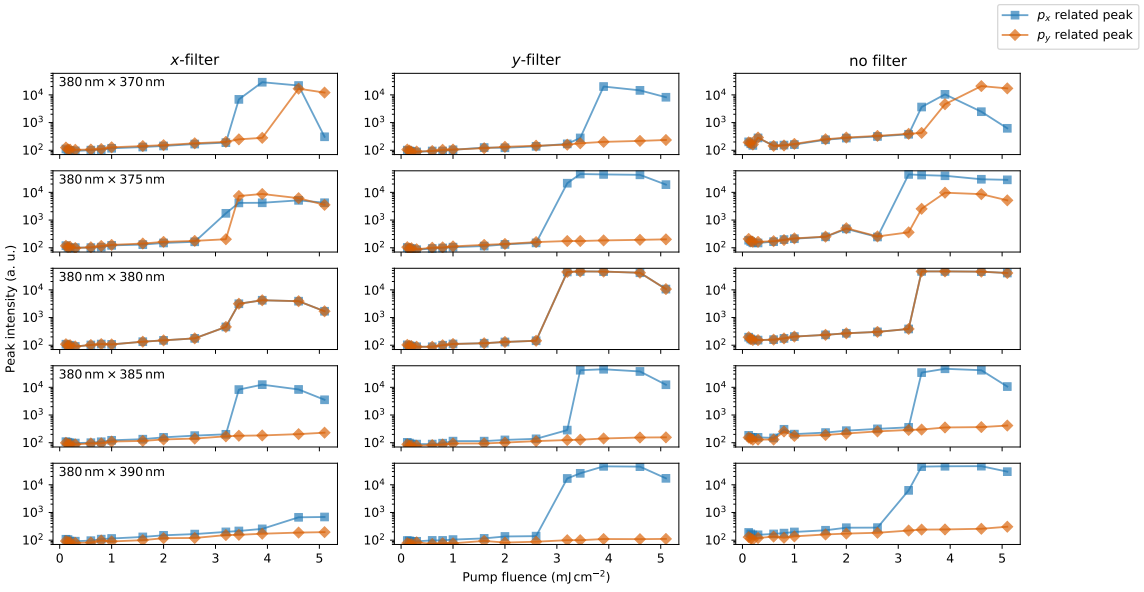


Figure S5: Maximum intensity of $p_x$ and $p_y$ related lasing peaks for different Ni nanodisk arrays and filter settings as a function of pump fluence.

array at all fluences, the lasing output with $x$ polarization is reduced. In line with the experimental observations, the numerical model predicts that quadrupolar and dipolar modes can contribute to the $p_x$ related lasing peak (see Figure 4 in the main text). The extent to which these different modes contribute to lasing depends on the variation of mode dynamics, available gain, and Q-factors with particle periodicity and pump fluence. We note that absolute values of lasing intensities in different arrays or polarization measurements are not directly comparable due to dye bleaching and other experimental factors.

# References


1. Hakala, T. K.; Rekola, H. T.; Väkeväinen, A. I.; Martikainen, J.-P.; Nečada, M.; Moilanen, A. J.; Törmä, P. Lasing in Dark and Bright Modes of a Finite-Sized Plasmonic Lattice. *Nat. Commun.* **2017**, *8*, 13687.